

On the Potential of Wireless Sensor Networks for the In-Situ Leaf Area Index Assessment using Gap Fraction Analysis

Jan Bauer^{a,*}, Bastian Siegmann^b, Thomas Jarmer^b, Nils Aschenbruck^a

^a University of Osnabrück, Institute of Computer Science,
Albrechtstr. 28, 49076 Osnabrück, Germany

^b University of Osnabrück, Institute for Geoinformatics and Remote Sensing,
Barbarastr. 22b, 49076 Osnabrück, Germany

Abstract

1 A precise and fine-grained in-situ monitoring of bio-physical crop parameters is
2 crucial for the efficiency and sustainability in modern agriculture. The leaf area
3 index (LAI) is an important key parameter, which allows to derive vital crop
4 information. As it serves as a valuable indicator for yield-limiting processes,
5 it contributes to situational awareness ranging from agricultural optimization
6 to global economy. This paper presents a feasible, robust, and low-cost modi-
7 fication of commercial off-the-shelf photosynthetically active radiation sensors,
8 which significantly enhances the potential of Wireless Sensor Network (WSN)
9 technology for the non-destructive in-situ LAI assessment. In order to minimize
10 environmental influences such as direct solar radiation and scattering effects,
11 we upgrade such a sensor with a specific diffuser combined with an appropriate
12 optical band-pass filter. We validate our approach in various field campaigns,
13 analyze the accuracy of bio-physical crop characteristics derived from WSN
14 data, and evaluate the robustness of our sensor modification.

Keywords: Wireless Sensor Network, Precision Agriculture, Crop Parameter,
Gap fraction, Leaf area index, LAI-2200.

^{*}Corresponding author. Tel.: +49 541 969 7167; fax: +49 541 969 2799.

Email addresses: bauer@uos.de (Jan Bauer), bsiegmann@igf.uos.de (Bastian Siegmann), tjarmer@igf.uos.de (Thomas Jarmer), aschenbruck@uos.de (Nils Aschenbruck)

15 **1. Introduction**

16 The Climate change and the increasing world population pose serious chal-
17 lenges to the primary economic sector as a whole and, in particular, to agri-
18 culture. Crop types, fertilization, irrigation, and crop protection have to be
19 adapted to changing conditions. An earlier and more precise situational aware-
20 ness of the status of agricultural fields is crucial for agricultural management
21 and could, moreover, improve the prediction of yield rates. For the realization of
22 a spatial fine-grained and timely situational awareness, there is a high demand
23 for in-situ exploration of bio-physical and bio-chemical crop characteristics by
24 advanced sensor technology.

25 In this context, the leaf area index (LAI) is one of the most important bio-
26 physical plant parameters and an indispensable factor in climatological, me-
27 teorological, ecological, and agricultural modeling. (Asner et al., 2003). It is
28 a valuable indicator and an integrative measure for the photosynthetic perfor-
29 mance of plants. Since the LAI provides important information for yield models,
30 it also serves as an indicator for yield-reducing processes caused by diseases or
31 mismanagement (Carter, 1994; Boegh et al., 2002). For flat-leaf vegetation,
32 Jonckheere et al. (2004) define the LAI as the ratio of the on-sided foliage area
33 to the ground surface area (m^2/m^2).

34 In the recent years, various methods for the LAI assessment have been de-
35 veloped. The *destructive* assessment of LAI usually provides the most precise
36 results, but is time-consuming, expensive, and, therefore, often limited to small
37 areas (Bréda, 2003; Jonckheere et al., 2004). Diverse methods of *non-destructive*
38 (also referred to as indirect) LAI assessment exist. On the one hand, the LAI can
39 be estimated in-situ. Jonckheere et al. (2004) and Weiss et al. (2004) provide a
40 comprehensive survey on common in-situ methodologies. An intercomparison of
41 these methods comprising digital hemispherical photography (DHP) (e.g., Ryu
42 et al., 2012; Francone et al., 2014) and specific handheld instruments, which
43 measure the solar transmittance of plant canopy (gap fraction analysis) (e.g.,
44 AccuPAR, SunScan, or LAI-2200) is given by Wilhelm et al. (2000) and Gar-

rigues et al. (2008). On the other hand, the LAI assessment derived from remote sensing images (airborne or satellite) represents an established non-destructive alternative (e.g., Boegh et al., 2002; Jarmer, 2013). However, common drawbacks of all assessment methods are their relatively low temporal and/or spatial resolution as well as the required (monetary) effort.

Wireless Sensor Networks (WSNs) comprise a large number of small, low-cost, and low-power sensor devices wirelessly interconnected in a self-organizing manner (Akyildiz et al., 2002). The primary task of each individual device within such a network is environmental sensing of physically measurable parameters, e.g., temperature, humidity, or ambient light. Beyond this data acquisition, the device is responsible for data transmission and forwarding to a central base station, possibly connected to the Internet. As WSNs are designed for large-scale and long-term deployments, sensor devices are highly resource-constrained (Anastasi et al., 2009) and, thus, have limited sensing accuracy. However, this limitation is compensated by the large number of collaborating devices, which are able to continuously provide sensor information at high temporal as well as spatial resolution. Hence, WSNs are tailored for in-situ monitoring of crop parameters as has been realized by research in the context of smart farming since one decade, cf. Langendoen et al. (2006). A promising progress has already been made in this area (e.g., Yuan et al., 2009; Bauer et al., 2014; Qu et al., 2014b). Eventually, WSNs have the potential to reduce time and labor costs of conventional in-situ acquisition and to beneficially assist the validation of parameter maps derived from remote sensing data.

In this paper, we continue our previous approach (Bauer et al., 2014) of non-destructive in-situ LAI assessment. We present a novel low-cost sensor modification which significantly enhances the investigated potential in terms of accuracy and robustness. Moreover, we evaluate the benefit of our approach in various field campaigns. At the same time, we turn our attention to its feasibility in practice. The core contributions of this paper are:

74 • the design of a novel low-cost sensor modification,
75 • six extensive field campaigns including comparative analyses, and
76 • an evaluation showing the impact of our approach.

77 **2. Related Work**

78 First preliminary experiences gained with an in-situ WSN deployment in
79 the area of precision agriculture are shared by [Langendoen et al. \(2006\)](#). The
80 authors report many engineering difficulties of large-scale and long-term deploy-
81 ments and create a foundation for future WSN research. Pioneer research in the
82 special domain of non-destructive LAI assessment based on WSN technology is
83 presented by [Yuan et al. \(2009\)](#). The authors propose an iterative scheme to
84 deploy sensors into farmland and apply statistical filters to the raw sensory data
85 in order to cope with variations of light reflection and refraction. Nonetheless,
86 they do not take advantage of any optical filter or diffuser. A continuous LAI
87 monitoring WSN is proposed by [Shimojo et al. \(2013\)](#) and demonstrated us-
88 ing commercial off-the-shelf (COTS) sensor nodes in a tomato greenhouse. The
89 authors emphasize that diffuse light conditions are crucial for the LAI assess-
90 ment based on gap fraction analysis. Hence, a diffusing hemispherical plastic
91 cover is used on top of each sensor. LAINet ([Qu et al., 2014b](#)) represents an-
92 other holistic WSN for agricultural LAI monitoring. Recently, [Qu et al. \(2014a\)](#)
93 focused on the in-situ assessment of the clumping index, which is closely re-
94 lated to the LAI. Moreover, the authors presented details of MLAOS, a custom
95 multi-point optical sensor system, which provides the basis of LAINet. MLOAS
96 uses optical diffusers and band-pass filters in order to minimize the influence of
97 scatter light.

98 In our previous work ([Bauer et al., 2014](#)), we investigated the LAI accuracy
99 achieved by a COTS sensor platform by conducting a direct comparison of WSN
100 results and values obtained by conventional standard instrumentation, namely
101 the LAI-2200 (LI-COR Inc., USA). Moreover, we suggest the *view pipe* concept

102 as simple modification of the optical sensor, which is shown to significantly
103 improve the correlation between both devices and, thus, the potential of WSNs.
104 However, this approach requires multiple sensors with multiple view pipes, which
105 hinders the use of a COTS sensor platform and its practicability. Following our
106 previous approach, our general goal is a feasible low-cost sensing system with
107 sufficient accuracy.

108 In this paper, we reuse the chosen sensor platform. Again, we validate the
109 achieved accuracy by a correlation analysis with the LAI-2200 (LI-COR, 2011)
110 as also done by Qu et al. (2014b). With regard to the sensor unit, MLAOS (Qu
111 et al., 2014a) is most related with our approach. However, we consider a different
112 range in the solar spectrum and achieve feasible results with a single COTS
113 sensor.

114 3. Background

115 3.1. Theoretical Background

116 In the visible (VIS) region of the electromagnetic spectrum (390–770 nm),
117 spectral reflectance and transmittance of vegetation are dominated by the im-
118 pact of pigments, e.g., chlorophyll and carotenoids (Gitelson et al., 2002). Due
119 to the fact that green vegetation strongly absorb the energy of radiation in the
120 range of blue (400–500 nm) and red light (600–700 nm) in order to carry out
121 photosynthesis, reflectance and transmittance in these ranges are on a very low
122 level, whereas being higher in the in the green domain (500–600 nm). This effect
123 is known as the so-called green peak. In the near infrared (NIR) region (700–
124 1400 nm), resulting from the cell structure, reflectance and transmittance first
125 highly increase, while then remain on a high level which greatly reduces the NIR
126 absorption (Gausman and Allen, 1973). Such a typical vegetation reflectance
127 spectrum is visualized in Figure 1 which shows an exemplary spectrum for maize
128 (*Zea mays L.*) measured in-situ with an ASD FieldSpec III (ASD Inc., USA)
129 spectroradiometer as well as a wheat (*Triticum aestivum L.*) spectrum acquired
130 by a SVC 1024i (Spectra Vista Corporation, USA) spectroradiometer.

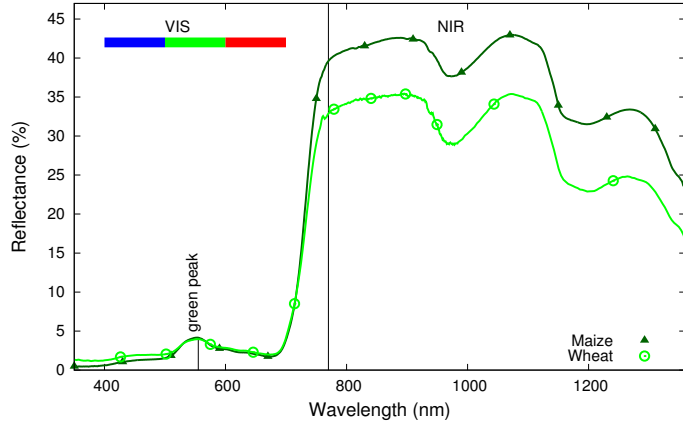


Figure 1: Typical reflectance spectrum curves of crops (maize and wheat) in the VIS and NIR region of solar radiation gathered by in-situ spectroradiometer measurements.

131 The properties of light transmittance of plants in the VIS spectrum is lever-
 132 aged by the indirect LAI determination which is based on the quantitative in-
 133 teraction between solar radiation and plant canopy, cf. [Jonckheere et al. \(2004\)](#).
 134 The *Monsi-Saeki model* ([Monsi and Saeki, 2005](#)), as used by [Yuan et al. \(2009\)](#),
 135 [Shimojo et al. \(2013\)](#), and [Bauer et al. \(2014\)](#), applies the well-known *Beer-*
 136 *Lambert* law for assessing the LAI (L). It results in

$$L = -\frac{1}{C} \ln \left(\frac{B}{A} \right), \quad (1)$$

137 where A is the light intensity observed above-canopy, B the corresponding inten-
 138 sity below-canopy, and the cultivar-specific term C . This term is the so-called
 139 *extinction coefficient*. It is given by the quantity of the specific light absorption
 140 property of plant's foliage and depends on various factors such as the leaf ori-
 141 entation angle. Moreover, the solar altitude has an significant impact on this
 142 coefficient. Please refer to [Monsi and Saeki \(2005\)](#) or [Jonckheere et al. \(2004\)](#)
 143 for further details.

144 The ratio of B to A represents the *transmittance*, which is gathered by
 145 standard optical instruments. These devices usually focus on a special spectral
 146 range within the VIS region where reflectance and transmittance of foliage is
 147 relatively low, e.g., in the range of blue light, cf. Figure 1. By doing so, the

148 maximum contrast between leaf and sky is achieved (Jonckheere et al., 2004).
 149 However, it is recommended to measure the light intensity under fully diffused
 150 sky conditions to cope with scattered radiation from leaf surfaces. Indeed, there
 151 exist more sophisticated approaches to remove the scattered radiation effect
 152 and provide an opportunity for LAI measurements even under sunny weather
 153 conditions, e.g., Kobayashi et al. (2013), as well as practical approaches tackling
 154 the challenge of scattered radiation, e.g., Qu et al. (2014a).

155 *3.2. Standard Instrumentation*

156 Reliable ground truth LAI values are very difficult to obtain. Only destruc-
 157 tive measurements provide high accuracy and precision, but are time-consuming
 158 and cost-intensive and, thus, sparsely conducted. Nonetheless, depending on
 159 the agricultural application, in-situ non-destructive solutions may achieve a suf-
 160 ficient accuracy. The LAI-2200 instrument, for instance, is one of the standard
 161 measuring devices for the non-destructive LAI assessment and widely used in
 162 agricultural research. We hence use the LAI-2200 in order to validate the LAI
 163 results gathered by WSN devices.

164 The LAI-2200 instrument consists of a measurement wand with a fish-eye
 165 optical sensor and a handheld control unit. The sensor's field of view is divided
 166 into five rings. For each ring i , a usual measurement of the LAI-2200 consists of
 167 a number (N_{obs}) of above (A_{ij}) and below canopy readings (B_{ij}). The former
 168 measure the total incoming light intensity above the canopy and the latter the
 169 residual incoming light which is neither reflected nor absorbed by the canopy.

170 Thereby, according to LI-COR (2011), the LAI (L) can be approximated with

$$L = 2 \sum_{i=1}^5 \overline{K_i} W_i, \text{ with } \overline{K_i} = \frac{1}{N_{obs}} \sum_{j=1}^{N_{obs}} \frac{-\ln \left(\frac{B_{ij}}{A_{ij}} \right)}{S_i}. \quad (2)$$

171 The factors W_i and S_i are specific weightings for the individual rings. For more
 172 details, please refer to LI-COR (2011).

173 **4. Measurement Architecture**

174 The practical meaning of Equations 1 and 2 in Section 3 is that a pair of
175 optical sensors (one above and one below the canopy) allow the LAI assessment.
176 Hence, our long-term vision is a continuous WSN deployment for in-situ crop
177 monitoring comprising a few sensors above the canopy as reference stations and
178 plenty of sensors below the foliage, similar to the implementation of LAINet (Qu
179 et al., 2014b). However, as a start of our research, our initial goal is a COTS
180 sensor enhancement with sufficient accuracy and robustness concerning LAI
181 estimation in practice. Therefore, we use the same architecture as presented by
182 Bauer et al. (2014), which is briefly described in the remainder of this section.

183 For the validation of our approach and the evaluation of the achieved ac-
184 curacy, we perform a comparative analysis with the LAI-2200. Regarding the
185 correlation between both devices, their similar positioning and orientation is a
186 crucial requirement for reliable and comparable results. Hence, in order to ex-
187 clude such potential error sources and inaccuracies resulting from instrumental
188 errors when using a pair of sensor nodes, we limit our measurement setup to
189 a single node, directly mounted onto the measurement wand of the LAI-2200.
190 Thus, we use the same sensor node for above and below data acquisition, simul-
191 taneously to the corresponding acquisition of the LAI-2200. Nevertheless, the
192 gathered sensor data still is transmitted to a fully-equipped device as central
193 instance for LAI computation, logging, and visualization. To this end, we use
194 the smartphone application introduced by Bauer et al. (2014).

195 *4.1. Hardware Components*

196 After various tests with diverse IEEE 802.15.4 (Baronti et al., 2007; IEEE,
197 2011) compliant COTS sensor platforms regarding their capabilities for the LAI
198 assessment based on gap fraction analysis, we came to the conclusion that the
199 TelosB¹ sensor platform (Memsic, USA), which is also used by Shimojo et al.

¹http://www.memsic.com/userfiles/files/Datasheets/WSN/telosb_datasheet.pdf

200 (2013), is greatly suited for our purpose (Bauer et al., 2014). Among its en-
201 vironmental sensors (temperature, humidity, and light), it features a photosyn-
202 thetically active radiation (PAR) sensor (Hamamatsu S1087), which covers the
203 desired spectral response rage from 320 to 730 nm with a peak sensitivity at a
204 wavelength of 560 nm. In particular under natural light conditions, we evaluated
205 this sensor as highly applicable for our purpose.

206 *4.2. Software Components*

207 The software framework consists of a data acquisition application running
208 on the TelosB platform and an LAI determination and visualization application
209 on the fully-equipped device, e.g., a smartphone. We implemented the data
210 acquisition application using TinyOS 2.1.2²(Levis et al., 2005), a widespread
211 open source operating system for low-power wireless devices, with a reasonable
212 memory footprint remaining enough memory for time synchronization (Römer
213 et al., 2005), data aggregation (Fasolo et al., 2007), routing algorithms (Akkaya
214 and Younis, 2005), and energy optimizations (Anastasi et al., 2009), which are
215 currently not yet integrated in our application. Since we do not only gather the
216 VIS light intensity perceived by the PAR sensor, but also monitor the temper-
217 ature and humidity for future purposes, we achieve a sampling rate of roughly
218 3 Hz. Details can be found in Bauer et al. (2014).

219 The LAI computation is performed by a fully-equipped device because the
220 data has to be filtered and fused, in particular in case of distributed sensors (as
221 in the intended WSN deployment). Thus, the readings of each individual sensor
222 are transmitted to that device. We combine (temporarily buffered) readings
223 in a batch of 17 samples per packet in order to utilize the maximum packet
224 size of IEEE 802.15.4. These packets are broadcasted with a rate of roughly
225 10 packets/min. Indeed, a more sophisticated, sparse, and energy-efficient sensor
226 data transmission would be required for a long-term deployment which is part
227 of our future work.

²<http://www.tinyos.net>

228 The central data sink application that receives these broadcasts averages the
 229 readings of each individual PAR sensor. In order to mitigate varying small-scale
 230 environmental noise, in our field campaigns, we take the mean of all 51 sensor
 231 samples included in three consecutive data packets (denoted by \bar{A} and \bar{B}). Using
 232 the means, the transmittance is determined. Finally, the LAIs of individual
 233 pairs of sensors are estimated according to Equation 2 (Section 3.2). As it is
 234 not possible to differentiate the angle of incoming light with a single COTS
 235 sensor, we cannot divide the field of view in rings as done by the LAI device of
 236 LI-COR. Instead, we rely on an averaged transmittance which results in:

$$L = 2 \sum_{i=1}^5 \bar{K}_i W_i \text{ with } \bar{K}_i = \frac{-\ln\left(\frac{\bar{B}}{\bar{A}}\right)}{S_i}. \quad (3)$$

237 Adopting the weighting factors from LI-COR (2011), the LAI can be expressed
 238 with:

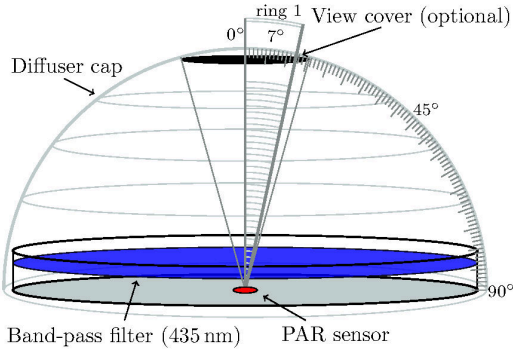
$$L = -\omega \cdot \ln\left(\frac{\bar{B}}{\bar{A}}\right), \quad (4)$$

239 where ω is roughly 1.2401 and contains the extinction coefficient mentioned
 240 in Section 3.1. Note that in our current measurement setup, which directly
 241 compares manually measured LAIs, we do not face large-scale noise, e.g., effected
 242 by wind or rain. Thus, more complex statistical filters as applied by Yuan et al.
 243 (2009) are not required here.

244 5. Design of a Sensor Enhancement

245 Bauer et al. (2014) introduced the *view pipe* approach, a simple, yet effective
 246 modification of the sensor's field of view, and demonstrated promising results.
 247 The idea is to imitate the individual rings in the visibility field of the LAI-2200
 248 instrument by adjusting the COTS sensor's field of view in a similar manner.
 249 Using a short pipe mounted onto the sensor, its lower (i.e., more horizontal)
 250 field of view is restricted. However, concerning its feasibility, the view pipe
 251 approach has an inherent drawback: In order to entirely map the five rings of

252 the LAI-2200's fish-eye sensor, five PAR sensors with corresponding view pipes
 253 would be necessary. Moreover, view pipes only restrict the lower bound of the
 254 visibility field.



(a) View cap concept: The diffusivity of incoming light is improved by an adequate diffuser cap, the spectral response range is restricted by a band-pass filter, and an optional view cover mitigates potential direct solar radiation from the zenith angle.



(b) Practical realization of the view cap concept: TelosB sensor node with a dark-blue band-pass filter (left) and an additional diffuser cap mounted on top of the filter (right).

Figure 2: Concept and realization of the sensor enhancement.

255 Due to this certain lack of feasibility, we reconsidered our previous approach
 256 and take a different direction. In our novel setup, referred to as *view cap* ap-
 257 proach, we take advantage of an optical diffuser in form of a hemispherical cap,
 258 following the approaches of Shimojo et al. (2013) and Qu et al. (2014a). How-

ever, based on previous experiences, the LAI accuracy (validated by comparative LAI-2200 results) is significantly impaired, if the sensor is not restricted somehow. Thus, we choose a restriction on a spectral level according to the black body assumption (LI-COR, 2011), which assumes a black foliage compared to the sky. This is achieved by an optical band-pass filter which rejects any incoming radiation with certain wavelengths in order to increase the contrast between foliage and sky and to mitigate scattering effects. Nonetheless, an additional restriction by an opaque cover that avoids direct sunlight from the zenith angle might be beneficial. Hence, we add an optional *view cover* at the top of the diffuser cap. This cover is designed to fade out the zenith visibility field ($0 - 10^\circ$) corresponding to the first ring of the LAI-2200 whose influence is also reduced to roughly 4 % by a small weighting factor, cf. (LI-COR, 2011). The overall concept of our new approach is depicted in Figure 2(a) and its practical realization is shown in Figure 2(b).

For the above mentioned spectral restriction, it is advisable to fade out the green peak in the reflectance spectrum of vegetation, cf. Section 3.1 and Figure 1. That could be easily realized by optical band-pass filters in the blue or red range of visible light. In contrast to Qu et al. (2014a), we decided to utilize a (low-cost) dark blue 435 nm band-pass filter (Baader Planetarium, Germany). The reason of this decision is that both reflectance and transmittance of vegetation in the blue spectrum is slightly lower than in the red spectrum, as exemplarily illustrated in Figure 3, that again visualizes the two reflectance spectrums from Figure 1 (maize and wheat), but in the specific spectral response range of the Hamamatsu PAR sensor. This characteristic of very low transmittance in the blue spectrum is advantageous concerning the black body assumption. Moreover, using the blue spectral range has the additional advantage that this region in the reflectance spectrum is only slightly changed under stress conditions, whereas red reflectance and transmittance is known to typically increase significantly (Slonecker, 2012). The LAI assessment based on a red band-pass filter might thus be prone to underestimation.

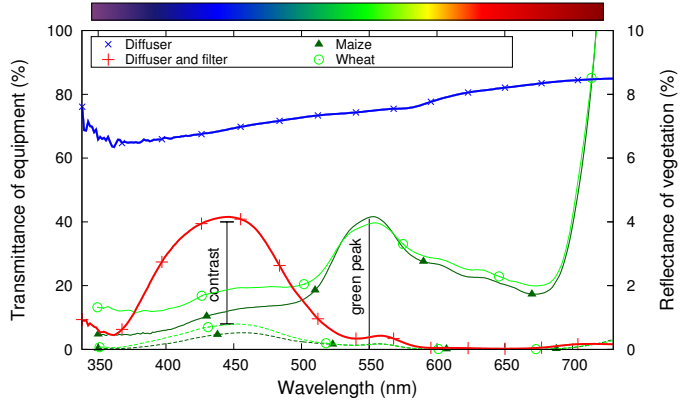


Figure 3: Spectral analysis of the transmittance (y1-axis) of the chosen diffuser with and without band-pass filtering within the spectral response range of the Hamamatsu S1087 sensor. Besides, reflectance spectrum curves of crops (maize and wheat) are shown on the y2-axis as measured in the field (solid line) and as perceived by the sensor after being filtered (dashed line).

Using the SVC 1024i (Spectra Vista Corporation, USA) spectroradiometer, we tested different diffusers in a laboratory environment and measured their transmittance as well as their transmittance in combination with the chosen band-pass filter. A detailed presentation of results are out of scope of this paper. However, a visualization of the properties of the selected diffuser are included in Figure 3. As the transmittance of the diffuser is relatively constant in the total response range of the PAR sensor and the diffuser does not decrease incoming radiation by more than roughly a third, it is suitable for LAI estimation. In addition, combining the diffuser with a dark blue band-pass filter, exactly the range of interest is passed. Moreover, considering the approximation of both plant reflectance curves perceived by the sensor after being filtered (dashed lines), the *green peak* (≈ 550 nm) is eliminated as intended. Finally, the transmittance and reflectance of vegetation is less than 10%, thus, offering a high contrast to the sky.

303 **6. Evaluation in Field Trials**

304 The goal of the field trials comprising six measurement campaigns in a maize
305 field (*Zea mays L.*) is to investigate the sensing accuracy of COTS sensor tech-
306 nology (TelosB) enhanced by the presented view cap concept. By a comparative
307 analysis with the results simultaneously measured by the LAI-2200 device, we
308 validate this accuracy and emphasize the potential of WSNs for a large-scale and
309 long-term agriculture deployment. We hope to achieve a similar accuracy and a
310 strong linear correlation between the LAI estimates derived from both devices.
311 Although the field measurements are exemplarily carried out in maize fields, we
312 are convinced that our sensing architecture is applicable to other flat-leaf crop
313 types. A validation of this assumption with various field campaigns in different
314 crop types is planned to be part of our future work.

315 *6.1. Study Area and Measurement Details*

316 The maize field which was investigated during the growing seasons 2014 and
317 2015 has a size of 3.5 ha and is located near the University of Osnabrück in the
318 north-western part of Germany. The mean annual precipitation of the area is
319 about 700 mm and the mean annual temperature between 8 and 9 °C.

320 Four maize measurement campaigns were carried out on July 23rd, Aug. 6th,
321 Aug. 21st, and Sept. 25th in 2014, two additional campaigns on Aug. 12th and
322 Aug. 20th in 2015. In every campaign, the LAI of 25–65 plots with seasonal
323 variations and different growth characteristics were measured to cover a wide
324 range of LAI values. In order to guarantee diffuse light conditions, which are a
325 basic prerequisite of the LAI-2200 device, all measurements were only conducted
326 either in the dawn between 6 am and 9 am ($0^\circ \leq \text{solar zenith angle} \leq 15^\circ$) or
327 between 9 am and 3 pm on days with a stable cloud cover ($15^\circ \leq \text{solar zenith}$
328 angle $\leq 55^\circ$).

329 In every campaign, the TelosB device was installed directly on the LAI-2200's
330 measurement wand, close to the fish-eye sensor. It simultaneously samples in-
331 coming radiation as described in Section 4.2 and periodically transfers its sensor
332 data to the fully-equipped device, which finally determines the LAI.

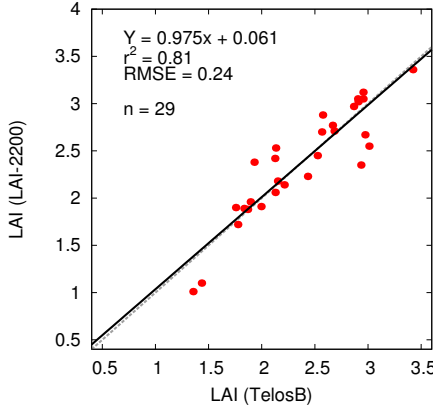


Figure 4: Comparison of LAI estimates by the enhanced TelosB sensor and LAI-2200 as reference in a first in-situ validation experiment (Campaign 1).

333 *6.2. Results*

334 As an initial proof of concept, we validated the basic setup (i.e., a sensor
 335 enhanced by diffuser and optical band-pass filter) in the first campaign. The
 336 comparative analysis of agreement between our setup and the LAI-2200 is shown
 337 in Figure 4 using a scatter plot. One can observe a clear linear relationship with
 338 a coefficient of determination (r^2) of 0.81 as well as a low root-mean-square
 339 error (RMSE) of 0.24. This initial result may seem similar to results of the
 340 view pipe approach proposed by [Bauer et al. \(2014\)](#). However, the latter results
 341 did not take the entire LAI-2200 visibility field into account, but only ring 1
 342 and 2 (hereinafter denoted as LAI23). Thus, the quality of the new approach
 343 is much more promising. Moreover, by adopting the weighting factors and
 344 the implicit extinction coefficient from the computation formulas of [LI-COR](#)
 345 ([2011](#)) (cf. Section 4.2), the LAI domains of both devices agree surprisingly
 346 well as the linear regression line is nearly overlapping the 1:1 line (dashed).
 347 Nevertheless, since the number of samples taken in this first campaign ($n = 29$)
 348 are insufficient to draw a sound conclusion, additional campaigns are required.

349 After the proof of our concept, we take a step backwards and quantitatively
 350 compare results from our previous concept (view pipes) with our new approach.
 351 Furthermore, we evaluate the impact of using an optical filter. Therefore, we

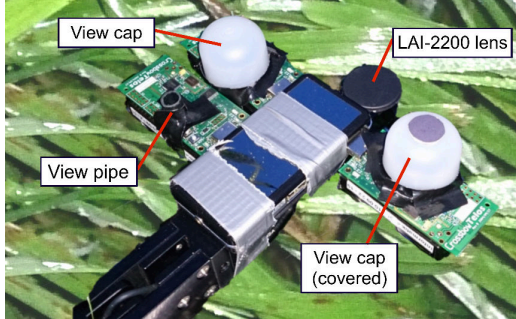


Figure 5: Measurement setup used for the comparative analysis of indirect LAI estimation using WSN devices with different approaches (view pipe and view cap concept (w and w/o view cover)) versus the conventional LAI-2200 methodology.

352 mounted TelosBs with different sensor modifications onto the LAI-2200 wand,
 353 as exemplarily illustrated in Figure 5. Although we might slightly loose prox-
 354 imity between the mounted sensors and the reference one, we thereby are able
 355 to perform all measurements simultaneously ensuring a spatiotemporal compa-
 356 rability.

357 The results are depicted in Figure 6. Both subfigures (a) and (b) concretize
 358 the weakness of the view pipe approach: Using a single sensor and a view pipe
 359 that limits its visibility according to the first two LAI-2200 rings, it is only
 360 possible to achieve an acceptable correlation ($r^2 = 0.67$, Figure 6(a)) regarding
 361 the corresponding LAI23 value (i.e., only ring 1 and 2 are used in the LAI-2200
 362 processing). Otherwise, the correlation is further decreased, represented by the
 363 lower coefficient of determination ($r^2 = 0.54$, Figure 6(b)).

364 Concerning our new approach, we investigated the impact of an optical filter.
 365 Figure 6(c) shows the poor performance ($r^2 = 0.14$, RMSE = 0.57) of the TelosB
 366 PAR sensor, if only a diffuser is used, but the perceived solar radiation is not
 367 filtered. In contrast, using the same setup with an optical filter integrated in the
 368 diffuser cap, we observe a significant increase of correlation with the reference
 369 device ($r^2 = 0.83$, RMSE = 0.26, Figure 6(d)). Thus, for the sensor's potential
 370 and the accuracy of our approach, the optical band-pass filter is an extremely
 371 important component of our architecture.

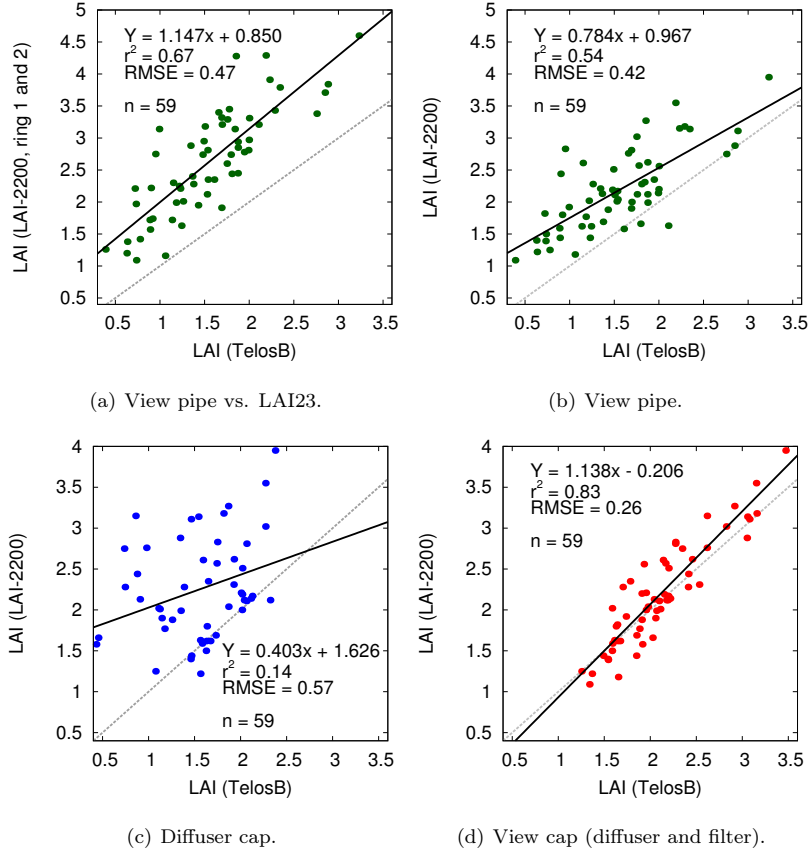


Figure 6: Comparison of LAI estimates using different modifications of TelosB sensors and LAI-2200 as reference (Campaign 2). LAI23 in (a) represents the LAI-2200 LAI estimate that corresponds to the visibility field of the view pipe (rings 3–5 are blocked in processing).

372 Besides the accuracy, the robustness of a measurement architecture against
 373 environmental influences is a relevant criteria for the potential of unattended
 374 long-term WSNs. Amongst others, the influence of direct sunlight is a crucial
 375 factor regarding the robustness and also a well-known source of error in the
 376 LAI-2200 architecture, which is applicable only at sunrise, sunset, or on cloudy
 377 days (LI-COR, 2011; Kobayashi et al., 2013). In order to evaluate the robustness
 378 of our approach with regard to direct sunlight, we took a closer look at the light
 379 intensity perceived by all modified sensors used in the second campaign (i.e.,

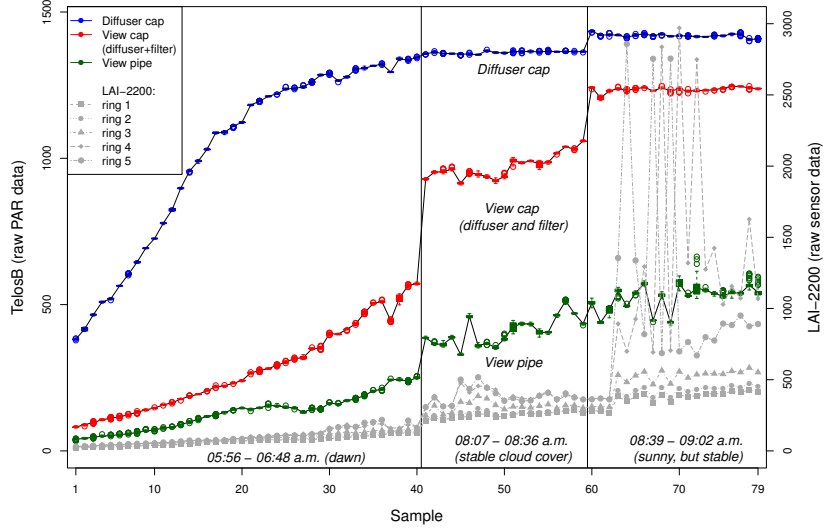


Figure 7: Intensity and variance of PAR measurements of different sensors gathered above canopy level in the second campaign. Both, the sequence of a sensor with a diffuser and in particular the sequence of a sensor with the view cap, show acceptable stability over time in all three phases, whereas the stability of the view pipe approach as well as the stability of the LAI-2200 (ring 4 and ring 5) suffer from direct radiation.

380 view pipe, diffuser cap, and view cap) during each above canopy measurement.
 381 The sequences of the gathered intensities of different sensors and also of each
 382 individual ring of the LAI-2200 instrument are shown in Figure 7.

383 Indeed, the sensitivity of individual sensors generally differ as expected be-
 384 cause of different setups which absorb incoming light in a different manner
 385 and/or because of individual fields of view. Note that each measurement sam-
 386 ple of the modified sensors represents the mean of 51 sensor readings (cf. \bar{A} in
 387 Section 4.2). These readings are visualized by confidence intervals in the figure,
 388 but hardly distinguishable due to negligible variances.

389 There were three different phases: a dawn phase (samples 1–40) with ideal
 390 environmental conditions, a stable cloud cover phase (samples 41–59) with ac-
 391 ceptable conditions, and a phase with sunny conditions (samples 60–79) baring
 392 the risk of direct radiation. Given stable environmental conditions, the se-
 393 quences of samples of each sensor are assumed to be stable as well. Hence,

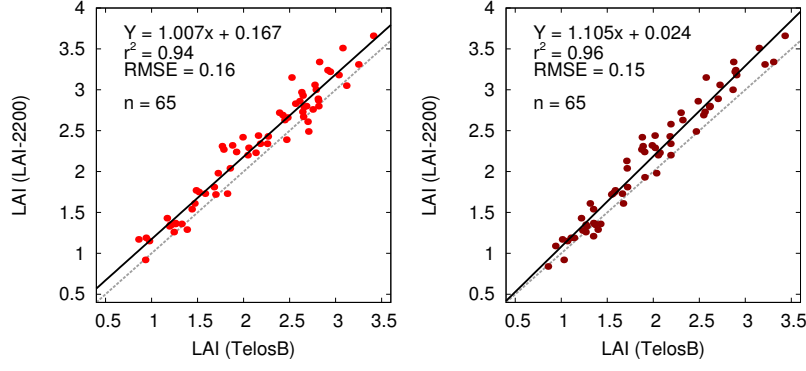


Figure 8: Comparison of LAI estimates using enhanced TelosB sensors and LAI-2200 as reference (Campaign 3 and 4).

394 during the first phase, a strictly monotonic increase of intensity sequence is
 395 expected due to the sunrise, whereas the sequences in the latter phases are ex-
 396 pected to result in a nearly steady state. However, the evaluation confirms that
 397 this expectation could not be achieved by conventional approaches. Figure 7
 398 emphasizes the high variance in the intensity sequences of the view pipe setup
 399 after the first phase as well as extreme outliers recorded by the LAI-2200 sensor,
 400 which is inoperative in direct sunlight (third phase) as predicted above. For this
 401 reason, the values measured in the third phase were excluded from the compar-
 402 ative analysis (cf. Figure 6). On the other hand, Figure 7 demonstrates that
 403 the diffuser approach tackles the challenge of direct sunlight since the diffuser
 404 sequence shows a smooth characteristic. As the variance only slightly in-
 405 creases when the diffuser is combined with the band-pass filter, our novel view
 406 cap approach enables the robustness required for an unattended deployment.

407 Finally, the benefit of the optional view cover intended to avoid potential
 408 inaccuracies by direct sunlight is investigated in Campaign 3 and 4. Figure 8
 409 shows the quality of the setup so far (a) and of the setup extended by the
 410 opaque view cover (b). In both cases, there is a substantial correlation with the
 411 reference device. However, the view cover is identified to result only in a minor

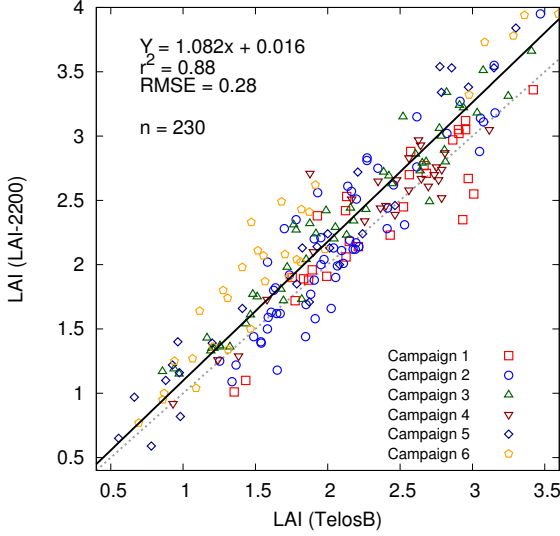


Figure 9: Comparison of the summarized LAI estimates of TelosB with view cap sensor enhancement and LAI-2200 in all maize campaigns.

improvement of the investigated correlation ($r^2 = 0.94$ to $r^2 = 0.96$). Though, by relying on the LAI-2200 comparison only and by neglecting more reliable destructive measurements, a general conclusion is hardly possible. Nevertheless, the cover does not seem to have a negative impact on the correlation on the other side. This result is very beneficial for the long-term unattended deployment in practice because dirt or dust particles might settle down on top of the diffuser cap and are expected to have a similar negligible impact.

6.3. Discussion

In conclusion, the estimates of both devices measured in all six field campaigns are compared in an overall scatter plot, cf. Figure 9. Note that a reasonable campaign-based clustering of estimates could not be observed since we considered different growth characteristics in each campaign and, thus, covered a wide range of LAI values each time.

Table 1: Performance of related approaches

| Approach | Technique | Species | Result (r^2) | Reference |
|----------------------------|-----------|---------|------------------|-------------|
| Ryu et al. (2012) | DHP | trees | 0.94 | LAI-2000 |
| Confalonieri et al. (2013) | DHP | rice | 0.97 | destructive |
| Francone et al. (2014) | DHP | grass | 0.86 | AccuPAR |
| | | maize | 0.92 | AccuPAR |
| | | reed | 0.88 | AccuPAR |
| Qu et al. (2014b) | WSN | maize | 0.27–0.97 | LAI-2000 |
| Bauer et al. (2014) | WSN | shrubs | 0.85–0.90 | LAI-2200 |

425 Figure 9 confirms the strong agreement of our approach with the reference
 426 instrument ($r^2 = 0.88$, RMSE = 0.28) and, thus, its appropriate accuracy. More-
 427 over, due to the extensive number of measured LAI values ($n = 230$) under dif-
 428 ferent seasonal and environmental influences as well as in various phenological
 429 stages, its robustness is implicitly demonstrated.

430 With regard to the related work, this strong and robust linear correlation
 431 can compete with results obtained by state-of-the-art approaches, which are ex-
 432 emplarily itemized in Table 1. The results generally are based on fewer measure-
 433 ment samples ($n \leq 30$) and, thus, do not provide information about their robust-
 434 ness. In contrast to these approaches, our novel sensor enhancement has the
 435 advantage of being simpler, yet more effective and cost-efficient. Compared to
 436 DHP approaches, no complex data processing is required, which demands more
 437 powerful and energy-consuming devices. On the other hand, no custom array
 438 of multiple sensors is necessitated as by related WSN approaches. Hence, our
 439 sensor enhancement increases the feasibility of low-cost and large-scale WSNs
 440 for the in-situ LAI assessment.

441 7. Conclusion

442 This paper presented a novel sensor approach based on COTS technology
443 that significantly enhances the potential of IEEE 802.15.4 WSNs for the in-situ
444 assessment of LAI, which is one of the most important metrics for bio-physical
445 crop characteristics. It was shown that our approach enables new opportunities
446 in terms of feasibility and robustness. Moreover, a comparative analysis re-
447 veals that substantial accuracy is achieved. Results are qualitatively comparable
448 with state-of-the-art results by specific commercial instruments (e.g., AccuPAR,
449 SunScan, and LAI-2200) and the complementary hemispherical photography ap-
450 proach, but enabled by small, low-cost, and energy-efficient devices.

451 In our future work, additional investigations in different crops are intended.
452 For that purpose, we will systematically conduct destructive LAI measurements
453 and occasionally process remote sensing data to widely validate our results.
454 Furthermore, we plan to deploy a long-term WSN prototype enabling LAI ac-
455 quisition with high spatiotemporal resolution.

456 Acknowledgments

457 This work was supported by the "Stifterverband für die Deutsche Wissenschaft"
458 (H170 5701 5020 20951).

459 References

460 Akkaya, K., Younis, M., 2005. A survey on routing protocols for wireless sensor
461 networks. *Ad hoc networks* 3 (3), 325–349.

462 Akyildiz, I. F., Su, W., Sankarasubramaniam, Y., Cayirci, E., Mar. 2002. Wire-
463 less Sensor Networks: A Survey. *Computer Networks* 38 (4), 393–422.

464 Anastasi, G., Conti, M., Francesco, M. D., Passarella, A., 2009. Energy conser-
465 vation in wireless sensor networks: A survey. *Ad Hoc Networks* 7 (3), 537 –
466 568.

467 Asner, G. P., Scurlock, J. M. O., A. Hicke, J., 2003. Global synthesis of leaf area
468 index observations: implications for ecological and remote sensing studies.
469 *Global Ecology and Biogeography* 12 (3), 191–205.

470 Baronti, P., Pillai, P., Chook, V. W., Chessa, S., Gotta, A., Hu, Y. F., 2007.
471 Wireless sensor networks: A survey on the state of the art and the 802.15.4
472 and ZigBee standards. *Computer Communications* 30 (7), 1655 – 1695.

473 Bauer, J., Siegmann, B., Jarmer, T., Aschenbruck, N., 2014. On the Potential
474 of Wireless Sensor Networks for the In-Field Assessment of Bio-Physical Crop
475 Parameters. In: Proc. of the 9th IEEE Int. Workshop on Practical Issues In
476 Building Sensor Network Applications (SenseApp). Edmonton, Canada, pp.
477 523–530.

478 Boegh, E., Soegaard, H., Broge, N., Hasager, C. B., Jensen, N. O., Schelde,
479 K., Thomsen, A., 2002. Airborne multispectral data for quantifying leaf area
480 index, nitrogen concentration, and photosynthetic efficiency in agriculture.
481 *Remote Sensing of Environment* 81 (2–3), 179–193.

482 Bréda, N., 2003. Ground-based measurements of leaf area index: a review of
483 methods, instruments and current controversies. *Journal of Experimental
484 Botany* 54, 2403–2417.

485 Carter, G. A., 1994. Ratios of leaf reflectances in narrow wavebands as indicators
486 of plant stress. *International Journal of Remote Sensing* 15 (3), 697–703.

487 Confalonieri, R., Foi, M., Casa, R., Aquaro, S., Tona, E., Peterle, M., Boldini,
488 A., Carli, G. D., Ferrari, A., Finotto, G., Guarneri, T., Manzoni, V., Movedi,
489 E., Nisoli, A., Paleari, L., Radici, I., Suardi, M., Veronesi, D., Bregaglio, S.,
490 Cappelli, G., Chiodini, M., Dominoni, P., Franccone, C., Frasso, N., Stella, T.,
491 Acutis, M., 2013. Development of an app for estimating leaf area index using a
492 smartphone. trueness and precision determination and comparison with other
493 indirect methods. *Computers and Electronics in Agriculture* 96 (0), 67 – 74.

494 Fasolo, E., Rossi, M., Widmer, J., Zorzi, M., April 2007. In-network aggregation
 495 techniques for wireless sensor networks: a survey. *Wireless Communications,*
 496 *IEEE* 14 (2), 70–87.

497 Francone, C., Pagani, V., Foi, M., Cappelli, G., Confalonieri, R., 2014. Com-
 498 parison of leaf area index estimates by ceptometer and PocketLAI smart app
 499 in canopies with different structures. *Field Crops Research* 155, 38–41.

500 Garrigues, S., Shabanov, N., Swanson, K., Morisette, J., Baret, F., Myneni, R.,
 501 2008. Intercomparison and sensitivity analysis of Leaf Area Index retrievals
 502 from LAI-2000, AccuPAR, and digital hemispherical photography over crop-
 503 lands. *Agricultural and Forest Meteorology* 148 (8–9), 1193–1209.

504 Gausman, H. W., Allen, W. A., 1973. Optical parameters of leaves of 30 plant
 505 species. *Plant Physiology* 52 (1), 57–62.

506 Gitelson, A. A., Zur, Y., Chivkunova, O. B., Merzlyak, M. N., 2002. Assessing
 507 Carotenoid Content in Plant Leaves with Reflectance Spectroscopy. *Photo-
 508 chemistry and photobiology* 75 (3), 272–281.

509 IEEE, 2011. IEEE Standard for Local and metropolitan area networks—Part
 510 15.4: Low-Rate Wireless Personal Area Networks (LR-WPANs).
 511 <http://standards.ieee.org/getieee802/download/802.15.4-2011.pdf>,
 512 checked: January 2016.

513 Jarmer, T., 2013. Spectroscopy and hyperspectral imagery for monitoring sum-
 514 mer barley. *International Journal of Remote Sensing* 34 (17), 6067–6078.

515 Jonckheere, I., Fleck, S., Nackaerts, K., Muys, B., Coppin, P., Weiss, M., Baret,
 516 F., 2004. Review of methods for in situ leaf area index determination: Part
 517 I. Theories, sensors and hemispherical photography. *Agricultural and Forest
 518 Meteorology* 121 (1–2), 19–35.

519 Kobayashi, H., Ryu, Y., Baldocchi, D. D., Welles, J. M., Norman, J. M., 2013.
 520 On the correct estimation of gap fraction: How to remove scattered radiation

521 in gap fraction measurements? Agricultural and Forest Meteorology 174–
522 175 (0), 170–183.

523 Langendoen, K., Baggio, A., Visser, O., 2006. Murphy loves potatoes: expe-
524 riences from a pilot sensor network deployment in precision agriculture. In:
525 Proc. of 20th Int. Parallel and Distributed Processing Symposium (IPDPS).
526 Rhodes Island, Greece.

527 Levis, P., Madden, S., Polastre, J., Szewczyk, R., Whitehouse, K., Woo, A.,
528 Gay, D., Hill, J., Welsh, M., Brewer, E., et al., 2005. Tinyos: An operating
529 system for sensor networks. In: Ambient intelligence. Springer, pp. 115–148.

530 LI-COR, 2011. LAI-2200 Plant Canopy Analyzer – Instruction Manual.
531 http://www.licor.co.za/manuals/LAI-2200_Manual.pdf, checked: Jan-
532 uary 2016.

533 Monsi, M., Saeki, T., 2005. On the Factor Light in Plant Communities and
534 its Importance for Matter Production. Annals of Botany 95 (3), 549–567
535 (originally published in German: Über den Lichtfaktor in den Pflanzenge-
536 sellschaften und Seine Bedeutung für die Stoffproduktion. Japanese Journal
537 of Botany, 1953).

538 Qu, Y., Fu, L., Han, W., Zhu, Y., Wang, J., 2014a. MLAOS: A Multi-Point Lin-
539 ear Array of Optical Sensors for Coniferous Foliage Clumping Index Measure-
540 ment. Sensors 14 (5), 9271–9289.

541 Qu, Y., Zhu, Y., Han, W., Wang, J., Ma, M., Feb 2014b. Crop Leaf Area Index
542 Observations With a Wireless Sensor Network and Its Potential for Validating
543 Remote Sensing Products. IEEE Journal of Selected Topics in Applied Earth
544 Observations and Remote Sensing 7 (2), 431–444.

545 Römer, K., Blum, P., Meier, L., 2005. Time synchronization and calibration
546 in wireless sensor networks. Handbook of sensor networks: Algorithms and
547 architectures 49, 199.

548 Ryu, Y., Verfaillie, J., Macfarlane, C., Kobayashi, H., Sonnentag, O., Vargas, R.,
549 Ma, S., Baldocchi, D. D., 2012. Continuous observation of tree leaf area index
550 at ecosystem scale using upward-pointing digital cameras. *Remote Sensing of*
551 *Environment* 126 (0), 116 – 125.

552 Shimojo, T., Tashiro, Y., Morito, T., Suzuki, M., Lee, D., Kondo, I., Fukuda,
553 N., Morikawa, H., 2013. A Leaf Area Index visualization method using wire-
554 less sensor networks. In: *Proc. of Int. Conf. on Instrumentation, Control,*
555 *Information Technology and System Integration Conference (SICE)*. Nagoya,
556 Japan, pp. 2082–2087.

557 Slonecker, T., 2012. Analysis of the effects of heavy metals on vegetation hyper-
558 spectral reflectance properties. In: Thenkabail, P., Lyon, J., Huete, A. (Eds.),
559 *Hyperspectral remote sensing of vegetation*. CRC, Ch. 23 *Analysis of the Ef-*
560 *fects of Heavy Metals on Vegetation Hyperspectral Reflectance Properties*,
561 pp. 561–578.

562 Weiss, M., Baret, F., Smith, G., Jonckheere, I., Coppin, P., 2004. Review of
563 methods for in situ leaf area index (LAI) determination: Part II. Estimation
564 of LAI, errors and sampling. *Agricultural and Forest Meteorology* 121 (1–2),
565 37 – 53.

566 Wilhelm, W., Ruwe, K., Schlemmer, M. R., 2000. Comparison of three leaf area
567 index meters in a corn canopy. *Crop Science* 40 (4), 1179–1183.

568 Yuan, Y., Li, S., Wu, K., Jia, W., Peng, Y., 2009. FOCUS: A cost-effective
569 approach for large-scale crop monitoring with sensor networks. In: *Proc. of*
570 *the Int. Conf. on Mobile Adhoc and Sensor Systems (MASS)*. Macao, China,
571 pp. 544–553.